to appear in Proc. IEEE/CIC ICCC

Performance Analysis of LoRa-Enabled Backscatter Communication

Abubakar S. Ali*, Shimaa Naser*, Omar Alhussein*†, and Sami Muhaidat *†

*Khalifa University 6G Research Centre, Abu Dhabi, UAE
†Department of Systems and Computer Engineering, Carleton University, Ottawa, Canada
engrabubakarsani@gmail.com, shimaa.naser@ku.ac.ae, omar.alhussein@ku.ac.ae, muhaidat@ieee.org

***Abstract*—Future wireless networks are evolving towards enabling reliable communications for miniature-sized and resource-constrained Internet-of-things (IoT) devices, imposing stringent requirements on the future sixth-generation (6G) mobile networks. These requirements include low cost, ultra-low latency, improved spectral and energy efficiencies, higher reliability, and significantly enhanced data rate. Emphasizing on the fact that these devices have limited capabilities and might be in inaccessible places, which make battery replacement or recharging a challenging task, energy-efficient solutions should be developed to ensure uninterrupted and seamless wireless communications for power-limited IoT devices. In this paper, we consider the integration of long-range (LoRa) modulation into backscatter communications (BackCom), and we develop a mathematical framework in order to investigate the error rate performance of the considered system model. In particular, we derive novel exact and approximated closed-form expressions for the symbol error rate (SER), under the assumption of canceled radio-frequency (RF) interference. The obtained analytical results, corroborated by numerical results, confirm the advantages of integrating LoRa into BackCom system as a low-complex technique in order to extend the transmission distance in power-limited backscatter devices.**

***Index Terms*—Backscatter communications, Deep Learning, IoT, LoRa, performance analysis.**

I. Introduction

With the evolution of advanced haptic application, and the emergence of five-senses wireless communications and human-computer interfaces, the role of the Internet-of-Things (IoT) paradigm becomes more vital in realizing such novel applications in future sixth generation (6G) wireless networks and beyond [1]. Despite their easy deployment, the short battery lifetime of IoT devices still constitutes a major design challenge, which requires a paradigm shift towards the development of the next generation green communication architecture. Backscatter communications (BackCom) have recently emerged as a new communications paradigm for low-power wireless networks. This approach is based on the concept that a transmitter sends data to its receiver by backscattering wireless signals, e.g., Wi-Fi signals [2]. BackCom promises to be an extremely low-power, cheaper, and simpler alternative to active low-power technologies. This is motivated by the fact that BackCom systems don't require expensive radio analog components, such as RF oscillators, crystals, and decoupling capacitors [3]]. Although BackCom systems are promising candidates for IoT networks, they suffer from several drawbacks, including low data rate, short-range communications, and dependence on the dynamics of wireless signals.

In this regards, low power wide area network (LPWAN) technologies have been identified as the underlying networks for IoT applications. This is attributed to their attractive features, including wide-range coverage, long battery life, and low data rates, that fit well in the context of low power IoT networks [4–7]. Long Range (LoRa), a branch of LPWAN is an emerging technology for low-power wireless communications, that operates in a non-licensed sub-GHz band with the aim to realize long-range communication, rendering it an enabler for BackCom.

LoRa-enabled BackCom has been recently proposed as an efficient mechanism to overcome short-range transmission limitations experienced in conventional BackCom systems. It is worthy to note that in conventional BackCom networks, the communication distance is limited to few meters. On the other hand, according to recent experimental studies [8–13], it was demonstrated that LoRa-enabled BackCom can enjoy a coverage of hundreds of meters, if not kilometers. In particular, in order to strike a balance between transmission range and throughput, the authors in [9] proposed a design for a low-power backscatter tag that piggybacks its symbols over LoRa transmission. In [10], the authors presented a wide-area backscatter system that is compatible with LoRa hardware to achieve reliable coverage across a 309 m^2 room. Ambuj and Carlos in [11] proposed LoRea with the purpose to improve the reliability of weak backscatter links to achieve an increased transmission range. PLoRa, an ambient backscatter design, was presented in [12] to enable long-range wireless communication by leveraging an ambient LoRa signal. To achieve long-range communication, employing a CSS modulation scheme, a modulator design that can backscatter different chirps was presented in [8]. In [13], a room-level localization technique was proposed to locate LoRa backscatter devices by exploiting the low-cost, low-power and long-range features of the underlying system. It should be highlighted that these contributions depend solely on experimental studies, and hence, lack a solid mathematical foundation, which is a necessity for system improvement purposes, and in order to allow better understanding to the integration of LoRa into BackCom systems.

In this paper, consider the integration of LoRa into BackCom systems, in which we extensively study the error rate

performance of the underlying system model. To the best of the authors' knowledge, such a framework has not been reported in the open literature yet.

The main contributions of this work are summarized as follows:

- We propose a thorough mathematical framework for the investigation of LoRa-enabled BackCom system, in which the backscattered signal is modeled as LoRa signal.
- Under the assumption of perfect cancellation of the radio frequency (RF) source signal, we analyze the error rate performance of LoRa-enabled BackCom, where we derive a novel approximate for the bit error rate (BER), over Rayleigh fading channels.

The rest of the paper is organized as follows: the considered system model is presented in Sec. II. Then, in Sec. III we present the correlator-based LoRa detector. Sec. IV presents the performance analysis of the considered system. Numerical and simulation results and discussions are presented in Sec. V. The paper is concluded in Sec. VI.

II. System Model

In this work, we consider an uplink LoRa-BackCom where a passive tag, empowered by an RF source (S), communicates with a receiver, as illustrated in Fig. 1. In particular, the RF source is assumed to be a unipolar signal generator, that generates single-tone unit-amplitude signals dedicated for BackCom purposes. The backscatter device operates on LoRa CSS modulation, in which chirp pulses are used to modulate the transmitted signals [14]. The achievable data rate of LoRa is determined by the spreading facor (SF), which specifies the number of bits transmitted in each LoRa symbol, SF $= 6, 7, \cdots, 12$ [15]. It should be noted that, the communication protocol and the system architecture of LoRa is defined by LoRaWAN, where LoRa defines the physical layer [15].

Now consider a narrow band system with center fequency f_c and bandwidth B, the passband single-tone signal from S can be expressed as

$$S(t) = s(t)e^{j(2\pi f_c t + \psi_c)}, \tag{1}$$

where $s(t)$ denotes the complex baseband signal representation of $S(t)$, and ψ_c represents the initial phase. The received signal at the tag can be expressed as

$$y_1(t) = g_1 S(t), \tag{2}$$

where g_1 is complex Gaussian channel coefficient between the RF source and the tag. The tag utilizes the received signal from S and performs LoRa modulation. Hence, the backscattered signal from the tag can be expressed as

$$c(t) = \rho b(t) y_1(t) e^{j(2\pi f_{LoRa} - \psi_{st})}, \tag{3}$$

where ρ is the tag reflection coefficient, f_{LoRa} represents the variable frequency corresponding to the baseband LoRa modulation, ψ_{st} is the phase offset between S and tag and $b(t)$ is the complex baseband LoRa waveform with equivalent discrete-time baseband signal given as [14–16]

$$b_k[n] = e^{j2\pi\left(\frac{n^2}{2N} + \left(\frac{k}{N} - \frac{1}{2}\right)\right)}, \tag{4}$$

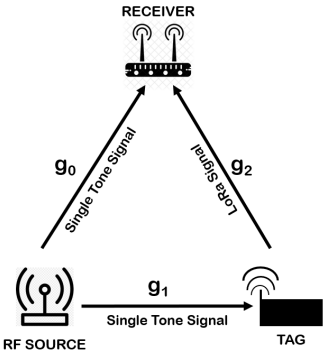

Fig. 1: LoRa-Enhanced BackCom System Model.

where $N = 2^{\text{SF}}$ is the total number of LoRa samples, $n = 0, 1, 2, \cdots, (N-1)$ is the sample index.

The backscattered signal is then transmitted to the LoRa receiver. Therefore the LoRa receiver receives a superposition of the RF source signal $S(t)$ and tag signal $c(t)$ which can be expressed as

$$y_r(t) = g_2 c(t) + g_0 S(t) + z_r(t), \tag{5}$$

where g_2 denotes the complex Gaussian channel coefficient between the tag and the reader with zero mean and unit variance, and $z_r(t)$ is the complex additive white Gaussian noise (AWGN) $\mathbb{CN}(0, \sigma^2)$ with $\sigma^2 = \frac{N_0}{2}$, and N_0 is the single-sided noise power spectral density.

Hence, the signal to interference plus noise ratio (SINR) can be expressed as

$$\gamma = \frac{E_s}{N \cdot N_0 + \sigma_i^2}. \tag{6}$$

where E_s depicts the LoRa symbol energy, and σ_i^2 is the RF interference power.

III. Correlator-Based Detector

Given that the backscattered signal is much weaker than the RF source signal, such interference can cause a severe degradation to the system performance. Inspired by the idea of direct link interference cancellation adopted in [10, 17], we aim to eliminate the effect of the RF source interference by introducing a small fixed frequency offset Δf to the backscattered LoRa signal. This will consequently transform the single-tone signal $S(t)$ into an out-of-band interference, that can be filtered by a band-pass filter [10]. Subsequently, the backscattered LoRa signal will be centered at $\Delta f + f_{LoRa}$. Therefore by inserting (3) and (4) into (5), and assuming a unit amplitude single-tone signal, the discrete-time received signal by the LoRa receiver can be rewritten as

$$y_r[n] = \rho g_1 g_2 e^{j2\pi\left(\frac{n^2}{2N} + \left(\frac{k}{N} - \frac{1}{2}\right)\right)} + z_r[n]. \tag{7}$$

Furthermore, with the RF source interference removed at the receiver, the SNR can therefore be expressed as

$$\gamma = \frac{E_s}{N \cdot N_0}. \tag{8}$$

Considering that the detection of LoRa signals relies on the orthogonality between the basis functions, a correlator can

be exploited to quantify the correlation between the received LoRa signal and the N basis functions [16]. Hence, the output of the correlator to detect the kth symbol can be obtained as follows

$$\sum_{n=0}^{N-1} y_r[n]\, x_i^*[n] = \begin{cases} \sqrt{\varrho E_s} + \phi_i, & i = k \\ \phi_i, & i \neq k \end{cases}, \tag{9}$$

where $x_i^*[n]$ is the complex conjugate of the i^{th} basis function, $\sqrt{\varrho} = |g_1|\,|g_2|$, and ϕ_i depicts the AWGN. In a non-coherent receiver, received LoRa symbols can be detected relying on an energy detector, in which the index of the detected symbol can be evaluated as

$$\tilde{k} = \arg\max_i \left(\left| \delta_{k,i} \sqrt{\varrho E_s} + \phi_i \right| \right), \tag{10}$$

where $\delta_{k,i} = 1$ when $i = k$ and 0, otherwise. Let $\tau_i = |\phi_i|$,

$$\tau_i = |z_r[n]|\,. \tag{11}$$

The computational complexity of (10) is $O(N^2)$ [14]. For simulation and application purposes, a discrete Fourier transform (DFT) based LoRa demodulation chain can be used to perform the demodulation [14]. This is an equivalent and low-complexity method with a computational complexity of $O(N\log N)$.

IV. Performance Analysis

In this section, we present the error rate performance analysis of LoRa-enabled BackCom system.

A. Exact Error Rate Performance Analysis of LoRa-enabled BackCom

The probability that a symbol k is erroneously received i.e., $i \neq k$ can be evaluated as

$$P_{e|\varrho} = \Pr\left[\max_{i, i\neq k} (\tau_i) > \beta_{k|\varrho} \right], \tag{12}$$

where $\beta_k = \left| \sqrt{\varrho P_r} + \phi_k \right|$ with $\phi_k = \frac{\phi_i}{N-1}$. From (12), it can be noticed that τ_i is a Rayleigh random variable. Therefore, the cumulative distribution function (CDF) of τ_i can be expressed as

$$F_{\tau_i}(x) = 1 - \exp\left[-\frac{x^2}{2\sigma^2} \right]. \tag{13}$$

On the other hand, $\tau = \max_{i, i\neq k}(\tau_i)$ depicts the maximum of $(N-1)$ i.i.d. Rayleigh random variables, and hence its CDF can be given as [16]

$$F\tau(x) = \left[1 - \exp\left[-\frac{x^2}{2\sigma^2} \right] \right]^{N-1}. \tag{14}$$

Similarly, β_k follows the Rician distribution with a joint probability distribution function (PDF) given by

$$f_{\beta_k}(x, \varrho) = \frac{x}{\sigma^2} \exp\left[-\frac{x^2 + \varrho E_s}{2\sigma^2} \right] I_0\left(\frac{x\sqrt{\varrho E_s}}{\sigma^2} \right) \cdot \Psi(\varrho), \tag{15}$$

where $I_0(\cdot)$ is the zeroth order modified Bessel function of the first kind. Given that $\sqrt{\varrho}$ follows a double Rayleigh distribution, its normalized channel power can be expressed as [18, 19]

$$\Psi(\varrho) = K_0(2\varrho) \tag{16}$$

where $K_0(\cdot)$ is the zeroth order modified Bessel function of the Second kind. By leveraging (15) and (16), the average symbol error rate (SER) of a LoRa symbol in the underlying system model can be evaluated as

$$P_{e|\varrho} = \int_0^\infty \int_0^\infty \left[1 - \left[1 - \exp\left[-\frac{x^2}{2\sigma^2} \right] \right]^{N-1} \right] f_{\beta_k}(x, \varrho) \mathrm{d}x \mathrm{d}\varrho. \tag{17}$$

Exploiting the binomial expansion theorem, the SER expression in (17) can be rewritten as

$$P_{e|\varrho} = \sum_{i=1}^{N-1} (-1)^{i+1} \binom{N-1}{i} \int_0^\infty \int_0^\infty \left[\exp\left[-\frac{x^2 i}{2\sigma^2} \right] \right] f_{\beta_{k|\varrho}}(x, \varrho) \mathrm{d}x \mathrm{d}\varrho. \tag{18}$$

By substituting (15) in (18), the conditional SER can be expressed as

$$P_{e|\varrho} = \sum_{i=1}^{N-1} (-1)^{i+1} \binom{N-1}{i} \int_0^\infty \left[\int_0^\infty \frac{x}{\sigma^2} \exp\left[-\frac{x^2(i+1) + \varrho E_s}{2\sigma^2} \right] I_0\left(\frac{x\sqrt{\varrho E_s}}{\sigma^2} \right) \mathrm{d}x \right] \cdot \Psi(\varrho) \mathrm{d}\varrho, \tag{19}$$

Evaluating the inner integral with respect to x, the conditional SER can be evaluated to

$$P_{e|\varrho} = \sum_{i=1}^{N-1} \frac{(-1)^{i+1}}{i+1} \binom{N-1}{i} \int_0^\infty \exp\left[-\frac{i\varrho\gamma N}{(i+1)} \right] \times \Psi(\varrho) d\varrho, \tag{20}$$

where γ was defined in (8). Using the integral table [20],

$$\int_0^\infty e^{-\Upsilon x} K_0(Cx)\, \mathrm{dx} = \frac{\arccos(\Upsilon/C)}{\sqrt{c^2 - \Upsilon^2}}, \tag{21}$$

where $C = 2$, and $\Upsilon = \frac{i}{i+1}\gamma N$. Hence, the symbol error rate can be expressed as

$$P_{e|\varrho} = \sum_{i=1}^{N-1} \frac{(-1)^{i+1}}{i+1} \binom{N-1}{i} \cdot \frac{\arccos(\Upsilon/C)}{\sqrt{c^2 - \Upsilon^2}}. \tag{22}$$

Assuming equiprobable symbols, and given that SF > 2, the average bit error (BER) is given as

$$P_b = \frac{2^{SF-1}}{N-1} \cdot P_e \approx 0.5 \cdot P_e. \tag{23}$$

B. Approximate Analysis of LoRa-enabled BackCom System

At high SF values, the binomial coefficient in (22) cannot be accurately evaluated using available simulation platforms, e.g., Matlab, Mathematica, MapleSoft, etc. Therefore, in this subsection, we derive an approximated, yet, accurate, expression for the BER of LoRa-enabled BackCom system. At high SNR values, the distribution of τ in (14) can be approximated as a Gaussian distribution with CDF represented as [39]

$$F_\tau(x) = \frac{1}{\sqrt{2\pi\sigma_\tau^2}} \exp\left[-\frac{(x - \mu_\tau)^2}{2\sigma_\tau^2} \right], \tag{24}$$

where μ_τ and σ_τ^2 are the mean and variance of τ respectively, given by [20]

$$\begin{aligned}\mu_\tau &= \left(\mu_\lambda^2 - \sigma_\lambda^2/2\right)^{1/4} \\ \sigma_\tau^2 &= \mu_\lambda - \left(\mu_\lambda^2 - \sigma_\lambda^2/2\right)^{1/2},\end{aligned} \tag{25}$$

with μ_λ and σ_λ^2 obtained as

$$\begin{aligned}\mu_\lambda &= 2\sigma^2 \cdot \sum_{i=1}^{m} \frac{1}{i} = 2\sigma^2 \cdot H_m \\ \sigma_\lambda^2 &= 4\sigma^4 \cdot \sum_{i=1}^{m} \frac{1}{i^2} \simeq 4\sigma^4 \cdot \frac{\pi^2}{6},\end{aligned} \tag{26}$$

where $m = N - 1$ and $H_m = \sum_{i=1}^{m} \frac{1}{i}$.

Furthermore, the PDF of β_k can be accurately approximated as a Gaussian random variable with PDF represented as

$$f_{\beta_{k|\varrho}}(x, \varrho) = \frac{1}{\sqrt{2\pi\sigma^2}} \exp\left[-\frac{\left(x - \sqrt{\varrho E_s}\right)}{2\sigma^2}\right] \cdot \Psi(\varrho), \tag{27}$$

Now let $\alpha = \tau - \beta_k$, the average BER can be expressed as

$$\begin{aligned}P_b &= 0.5 \times P_{e|\varrho} \\ &= 0.5 \times \Pr\left(\alpha > 0\right),\end{aligned} \tag{28}$$

Hence, the average BER can be expressed as

$$P_b = 0.5 \times \frac{1}{\sqrt{2\pi\sigma_\alpha^2}} \int_0^\infty \int_0^\infty \exp\left[-\frac{\left(x - \mu_\alpha\right)^2}{2\sigma_\alpha^2}\right] \cdot \Psi(\varrho) dx d\varrho, \tag{29}$$

where $\mu_\alpha = \mu_\tau - \sqrt{\varrho E_s}$ and $\sigma_\alpha^2 = \sigma_\tau^2 + \sigma^2$. By leveraging the definition of the Gaussian Q-function, the expression in (29) can be rewritten as

$$\begin{aligned}P_b &= 0.5 \times \int_0^\infty Q\left(\frac{-\mu_\alpha}{\sigma_\alpha}\right) \cdot \Psi(\varrho) d\varrho \\ &= 0.5 \times \int_0^\infty Q\left(\frac{\sqrt{\varrho E_s} - \mu_\tau}{\sqrt{\sigma_\tau^2 + \sigma^2}}\right) \cdot \Psi(\varrho) d\varrho,\end{aligned} \tag{30}$$

Hence, by inserting (25) into (30), and utilizing (16), the approximate BER expression can be expressed as

$$P_b = 0.5 \times \int_0^\infty Q\left(\frac{\sqrt{\varrho\gamma N} - \left[H_m^2 - \frac{\pi^2}{12}\right]^{0.25}}{\sqrt{H_m - \sqrt{H_m^2 - \frac{\pi^2}{12}} + 0.5}}\right) \cdot \Psi(\varrho) d\varrho. \tag{31}$$

It is demonstrated in [16] that the integral in (31) can be simplified to

$$P_b = 0.5 \times \int_0^\infty Q\left(1.28\sqrt{\varrho\gamma \cdot N} - 1.28\sqrt{SF} + 0.4\right) \cdot \Psi(\varrho) d\varrho. \tag{32}$$

Due to the mathematical intractability of (32), we resort to the approximation for the PDF of ϱ given by [21], its normalized channel power can be expressed as

$$\Psi(\varrho) = \varrho^{-0.25} e^{-2\varrho}. \tag{33}$$

Furthermore, we utilize the generalized Gauss-Laguerre Quadrature (GLQ) approach,

$$\int_0^\infty x^a e^{-x} f(x) dx \approx \sum_{q=1}^{z} u_q f(y_q), \tag{34}$$

where u_q and y_q are the respective weights and roots of the generalized GLQ [43]. Hence, the approximated expression of the average BER can be written as

$$P_b = 0.5 \sum_{q=1}^{z} u_q y_q^{-1.25} e^{-y_q} Q\left(1.28\sqrt{y_q\gamma \cdot N} - 1.28\sqrt{SF} + 0.4\right). \tag{35}$$

V. Results and Discussions

In this section, we present the numerical results, in order to corroborate the accuracy of the derived expressions in Section IV. Due to the precision limitations in mathematical platforms, e.g., Matlab, Mathematica, and MapleSoft, the accuracy of the derived expression in (23) will be validated through numerical results, for SF = 3, and 5. Furthermore, we will exploit the expression in (23) in order to corroborate the accuracy of the considered approximation in (35). Therefore, Fig. 2 plots the analytical BER expressions in (23) and (35), for SF = 3, and 5, and rho=1. The perfect agreement between the numerical and the exact analytical results, for all considered SF values and over the entire SNR range, confirms the validity of the exact SER expression derived in (23).

Furthermore, it can be noticed that the approximation utilized to generate (35) is tight, as it can be noticed from Fig. 3 that the BER difference between the exact performance and approximated one in (35) is negligible. This validates the correctness of the presented analytical framework in Sec. IV.

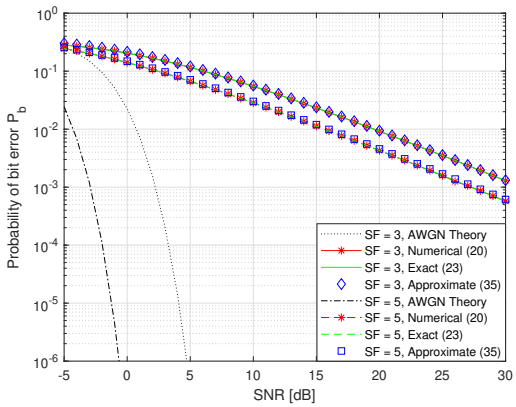

Fig. 2: The BER of LoRa-enabled BackCom, $SF = 3, 5$, and $\rho = 1$.

In Fig. 4, we compare the approximated SER of the underlying system model, with the corresponding simulation results, while considering more practical SF value, e.g., SF = 7, 8, and 9. It can be observed from Fig. 3 that the approximated analysis perfectly matches the simulation ones for the considered SF values and over the entire SNR range. This further confirms the validity of the proposed approximated analytical framework under the assumption of practical SF

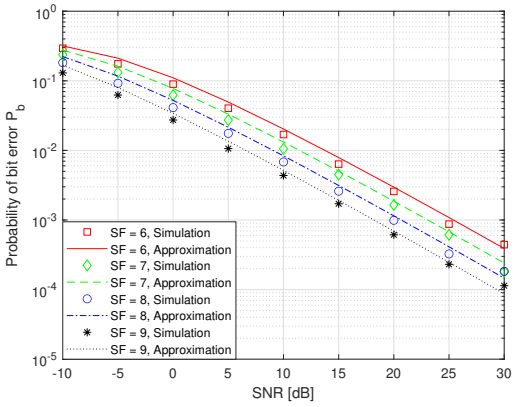

Fig. 3: Approximated SER and simulation results of Lora-enabled BackCom, SF = 7, 8, and 9, ρ =1.

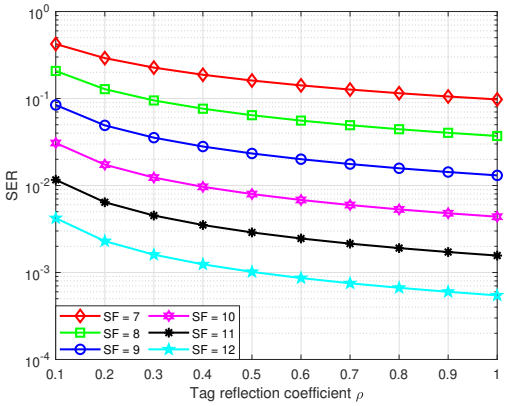

Fig. 4: LoRa-enabled BackCom BER performance vs Tag reflection coefficient, $\rho = 0, 0.1, \cdots, 1$ with $d_{st} = d_{tr} = 200m$.

values, and therefore, it can be reliably utilized to quantify the error rate performance of the considered system model.

With the aim to obtain more insights into the error rate performance of LoRa-enabled BackCom systems, we study the effect of the link distances on the performance of such systems. Without loss of generality, we assume that the transmission is performed over the 868 MHz band, with wavelength $\lambda = 34.54$ cm. Furthermore, we consider that the transmit power of S is $P_s = 20$ dBm, and the antenna gains of S, tag, and the LoRa receiver are set as $G_s = 8$ dB, $G_r = 2.2$ dB, and $G_r = 2.15$ dB, respectively. Therefore, using Friis free space propagation model [22], the received power of the backscattered signal at the LoRa receiver can be computed as

$$P_{rt} = \rho P_s G_s G_t^2 G_r K^2 d_{st}^{-a} d_{tr}^{-a}, \tag{36}$$

where $a = 2$ is the free-space pathloss exponent [23], d_{st} is the distance between S and the tag, and d_{tr} is the distance between the tag and the LoRa receiver. Hence, the average receive SNR in dB can be expressed as

$$\gamma = P_{rt} - P_{RX}, \tag{37}$$

where P_{RX} is the adaptive LoRa receiver sensitivity [24].

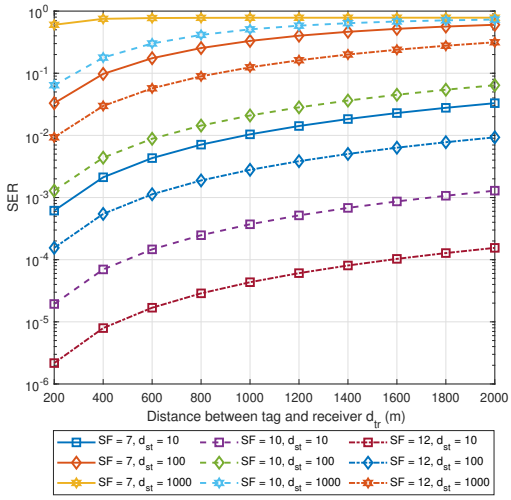

Fig. 5: LoRa-backscatter BER performance vs Distance between tag and receiver $d_{tr} = 200, 400, \cdots, 2000$m with $\rho = 1$.

Leveraging (37), the SER performance of the system is further evaluated for a wider range of backscatter tag attenuation coefficient, as shown in Fig. 4. It can be observed from Fig. 4 that ρ has a critical impact on the SER performance of LoRa-enabled BackCom systems. For example, as ρ goes from 0.1 to 1, the SER for SF = 12 drops from 4.2×10^{-3} to approximately 5.4×10^{-4}. This stimulates the importance of designing efficient tags that are capable of reflecting the maximum of the received power.

Fig. 5 shows the SER performance of the underlying system model versus the distance between the tag and the LoRa receiver. The results in Fig. 5 demonstrates the advantages of leveraging LoRa in BackCom systems, in order to extend the communication range. As reported in the literature, the typical communication range in BackCom is limited to few meters, and sometimes to less than 1 m. However, when integrating LoRa, it can be shown, as depicted in Fig. 5 that the communication distance can be extended to much wider ranges. In particular, it can be observed that, for SF = 12 approximately an SER of 10^{-4} can be achieved when the distance between the tag and reader equals to 1600 m, and the carrier emitter is placed 10m from the tag. This indicates that such an integration between LoRa and BackCom could be a paradigm shift towards realizing reliable, long distance, energy efficient wireless communications for resources-constrained IoT networks.

VI. Conclusions

In this paper, we have evaluated the error rate performance of LoRa-enabled BackCom system over Rayleigh fading channels. In particular, we derived accurate exact and approximated expressions for the error rate, and the accuracy of the analytical framework is validated through numerical results. When parameters are varied, the obtained results show that the system SER performance increases with increasing SNR. Also, we studied the impact of the tag reflection coefficient on the system performance, and it was demonstrated that, the

SER performance of the considered system model improves with increasing the tag reflection coefficient. It is further concluded that leveraging LoRa in BackCom systems can offer an improved performance when the transmission distance goes beyond the tens of meters.

REFERENCES

[1] L. Bariah, L. Mohjazi, S. Muhaidat, P. C. Sofotasios, G. K. Kurt, H. Yanikomeroglu, and O. A. Dobre, "A prospective look: Key enabling technologies, applications and open research topics in 6g networks," *IEEE Access*, vol. 8, pp. 174 792–174 820, 2020.

[2] N. Van Huynh, D. T. Hoang, X. Lu, D. Niyato, P. Wang, and D. I. Kim, "Ambient backscatter communications: A contemporary survey," *IEEE Commun. Surveys Tuts.*, vol. 20, no. 4, pp. 2889–2922, 2018.

[3] X. Kang, L. Y. C., and J. Yang, "Riding on the primary: A new spectrum sharing paradigm for wireless-powered IoT devices," in *Proc. IEEE Int. Conf. Commun. (ICC)*, vol. 2017-June, 2017, pp. 1–6.

[4] Q. M. Qadir, T. A. Rashid, N. K. Al-Salihi, B. Ismael, A. A. Kist, and Z. Zhang, "Low power wide area networks: A survey of enabling technologies, applications and interoperability needs," *IEEE Access*, vol. 6, pp. 77 454–77 473, 2018.

[5] S. Devalal and K. Iot, "LoRa technology-an overview," in *Proc. IEEE Int. Conf. Electron. Commun. Aerosp. Technol. (ICECA)*, no. Iceca. IEEE, 2018, pp. 284–290.

[6] A. Zourmand, A. L. Kun Hing, C. Wai Hung, and M. Abdulrehman, "Internet of Things (IoT) using LoRa technology," in *Proc. IEEE Int. Conf. Autom. Control Intell. Syst. (I2CACIS)*, no. June. IEEE, 2019, pp. 324–330.

[7] A. Muthiah, S. Ajitha, M. T. K. S, V. V. K, K. Kavitha, and R. Marimuthu, "Maternal ehealth Monitoring System using LoRa Technology," in *Proc. IEEE Int. Conf. Aware. Sci. Technol. (iCAST)*. IEEE, 2019, pp. 1–4.

[8] R. Correia, Y. Ding, S. N. Daskalakis, P. Petridis, G. Goussetis, A. Georgiadis, and N. B. Carvalho, "Chirp Based Backscatter Modulation," in *Proc. IEEE Int. Microw. Symp. Dig. (MTT-S)*, vol. 2019-June, 2019, pp. 279–282.

[9] X. Guo, L. Shangguan, Y. He, J. Zhang, H. Jiang, A. A. Siddiqi, and Y. Liu, "Aloba: Rethinking ON-OFF keying modulation for ambient LoRa backscatter," in *Proc. ACM Conf. Embed. Networked Sens. Syst. (SenSys)*, 2020, pp. 192–204.

[12] Y. Peng, L. Shangguan, Y. Hu, Y. Qian, X. Lin, X. Chen, D. Fang, and K. Jamieson, "PlorA: A passive long-range data network from ambient Lora transmissions," in *Proc. ACM Spec. Interest Group Data Commun. (SIGCOMM)*, 2018, pp. 147–160.

[10] V. Talla, M. Hessar, B. Kellogg, A. Najafi, J. R. Smith, and S. Gollakota, "LoRa backscatter: Enabling the vision of ubiquitous connectivity," in *Proc. ACM Interact. Mob. Wearable Ubiquitous Technol.*, vol. 1, no. 3, 2017, p. 24.

[11] A. Varshney, C. Pérez-Penichet, C. Rohner, and T. Voigt, "Towards wide-area backscatter networks," in *Proc. ACM Workshop Hot Top. Netw. (HotWireless)*, 2017, pp. 49–53.

[13] A. Lazaro, M. Lazaro, and R. Villarino, "Room-level localization system based on LoRa backscatters," *IEEE Access*, vol. 10, no. 1109, pp. 1–15, 2021.

[14] O. Afisiadis, M. Cotting, A. Burg, and A. Balatsoukas-Stimming, "On the Error Rate of the LoRa Modulation with Interference," *IEEE Trans. Wireless Commun.*, vol. 19, no. 2, pp. 1292–1304, 2020.

[15] C. F. Dias, E. R. D. Lima, and G. Fraidenraich, "Bit error rate closed-form expressions for LoRa systems under nakagami and rice fading channels," *Sensors (Switzerland)*, vol. 19, no. 20, pp. 1–11, 2019.

[16] T. Elshabrawy and J. Robert, "Closed-Form Approximation of LoRa Modulation BER Performance," *IEEE Commun. Lett.*, vol. 22, no. 9, pp. 1778–1781, 2018.

[17] Q. Tao, C. Zhong, K. Huang, X. Chen, and Z. Zhang, "Ambient Backscatter Communication Systems with MFSK Modulation," *IEEE Trans. Wireless Commun.*, vol. 18, no. 5, pp. 2553–2564, 2019.

[18] M. Uysal, "Diversity analysis of space-time coding in cascaded rayleigh fading channels," *IEEE Commun. Lett.*, vol. 3, no. 3, pp. 1471–1474, 2006.

[19] P. S. Bithas, K. Maliatsos, and A. G. Kanatas, "The Bivariate Double Rayleigh Distribution for Multichannel Time-Varying Systems," *IEEE Commun. Lett.*, vol. 5, no. 5, pp. 524–527, 2016.

[20] A. P. Prudnikov, Y. A. Brychkov, and O. I. Marichev, *Integrals and Series: Volume 2*, 1986, vol. 2.

[21] H. Lu, Y. Chen, and N. Cao, "Accurate approximation to the PDF of the product of independent rayleigh random variables," *IEEE Antennas Wireless Propag. Lett.*, vol. 10, no. 2, pp. 1019–1022, 2011.

[22] J. G. Proakis and M. Salehi, *Digital Communications*, 5th ed. The McGraw-Hill Companies, 2008.

[23] F. Palacio, R. Agustí, J. Pérez-Romero, M. López-Benítez, S. Grimoud, B. Sayrac, I. Dagres, A. Polydoros, J. Riihijärvi, J. Nasreddine, P. Mähönen, L. Gavrilovska, V. Atanasovski, and J. Beek, "Radio environmental maps: information models and reference model." *ICT-248351 FARAMIR*, pp. 1–95, July 2011.

[24] Semtech Corporation, "Understanding the LoRa Adaptive Data Rate," pp. 1–15, 2019.